ARTICLES

nature structural & molecular biology

Mechanism of transcriptional stalling at cisplatin-damaged DNA

Gerke E Damsma[1,2], Aaron Alt[1], Florian Brueckner[1,2], Thomas Carell[1] & Patrick Cramer[1,2]

The anticancer drug cisplatin forms 1,2-d(GpG) DNA intrastrand cross-links (cisplatin lesions) that stall RNA polymerase II (Pol II) and trigger transcription-coupled DNA repair. Here we present a structure-function analysis of Pol II stalling at a cisplatin lesion in the DNA template. Pol II stalling results from a translocation barrier that prevents delivery of the lesion to the active site. AMP misincorporation occurs at the barrier and also at an abasic site, suggesting that it arises from nontemplated synthesis according to an 'A-rule' known for DNA polymerases. Pol II can bypass a cisplatin lesion that is artificially placed beyond the translocation barrier, even in the presence of a G•A mismatch. Thus, the barrier prevents transcriptional mutagenesis. The stalling mechanism differs from that of Pol II stalling at a photolesion, which involves delivery of the lesion to the active site and lesion-templated misincorporation that blocks transcription.

Cisplatin (*cis*-diamminedichloroplatinum(II)) is a widely used anticancer drug that forms DNA adducts that interfere with replication and transcription[1]. The most frequent cisplatin DNA adducts are 1,2-d(GpG) intrastrand cross-links, or cisplatin lesions, in which platinum coordinates the N7 atoms of adjacent guanosines in a DNA strand[2] (**Fig. 1a**). A cisplatin lesion in the DNA template strand blocks transcription elongation by the single-subunit RNA polymerase from phage T7 (ref. 3) and by Pol II[4–6], and leads to stable polymerase stalling[7]. The stalled Pol II elongation complex can be bound by the elongation factor TFIIS, which stimulates polymerase back-tracking and 3′ RNA cleavage[6]. A small fraction of polymerases can apparently read through a cisplatin lesion[6].

The detailed molecular mechanisms of cisplatin DNA adduct processing by nucleic acid polymerases are not understood. Here we have used a combination of X-ray crystallography and RNA-extension assays to derive the molecular mechanism of *Saccharomyces cerevisiae* Pol II stalling at a cisplatin lesion. Comparison of the results with our previous analysis of Pol II stalling at a DNA photolesion, a TT cyclobutane pyrimidine dimer[8] (CPD, **Fig. 1a**), reveals that the two types of dinucleotide lesions trigger transcriptional stalling by different mechanisms.

RESULTS

Structure of a cisplatin-damaged Pol II elongation complex

To elucidate recognition of cisplatin-induced DNA damage by transcribing Pol II, we carried out a structure-function analysis of elongation complexes containing a cisplatin lesion in the template DNA strand. Elongation complexes were reconstituted from the 12-subunit *S. cerevisiae* Pol II and nucleic acid scaffolds as described[8,9]. A cisplatin lesion was first incorporated at registers +2/+3 of the template strand, directly downstream of the NTP-binding site at register +1 (scaffold A, **Fig. 1b**). The crystal structure of the resulting cisplatin-damaged elongation complex (complex A) was determined at 3.8-Å resolution (**Fig. 1c,d** and Methods). A very strong peak in the anomalous difference Fourier map revealed the location of the platinum atom (**Fig. 1c**).

In the damaged elongation complex structure, the cisplatin lesion is bound at positions +2/+3, above the polymerase bridge helix (**Fig. 1d**). The DNA-RNA hybrid occupies the upstream positions –1 to –8. The hybrid structure is essentially identical to our previous structures of the complete Pol II elongation complex[9] and the elongation complex containing a CPD lesion at the polymerase active site[8]. However, the downstream DNA duplex adopts a slightly altered position (**Fig. 1e**). The change in the downstream DNA position results from the presence of the cisplatin lesion rather than from the scaffold design or the nucleic acid sequences, which were highly similar to those used previously[8]. Structures of free DNA containing a cisplatin lesion[10,11] reveal that the lesion at the center of the duplex leads to DNA bending. In our structure, the lesion is located at the end of the duplex and induces a slight repositioning of the downstream DNA, without substantial changes in its internal structure.

RNA polymerase II stalling and AMP misincorporation

The crystal structure of complex A defines a state of the elongation complex in which the lesion lies downstream of the active site. We therefore used complex A in RNA-extension assays to investigate the mechanism of Pol II stalling. The RNA was labeled with a fluorescent dye at its 5′ end, complex A was incubated with NTP substrates, and

[1]Center for Integrated Protein Science CIPS[M], Department of Chemistry and Biochemistry, and [2]Gene Center Munich, Ludwig-Maximilians-Universität München, Feodor-Lynen-Strasse 25, 81377 Munich, Germany. Correspondence should be addressed to T.C. (thomas.carell@cup.uni-muenchen.de) or P.C. (cramer@LMB.uni-muenchen.de).

Received 12 June; accepted 18 September; published online 11 November 2007; doi:10.1038/nsmb1314

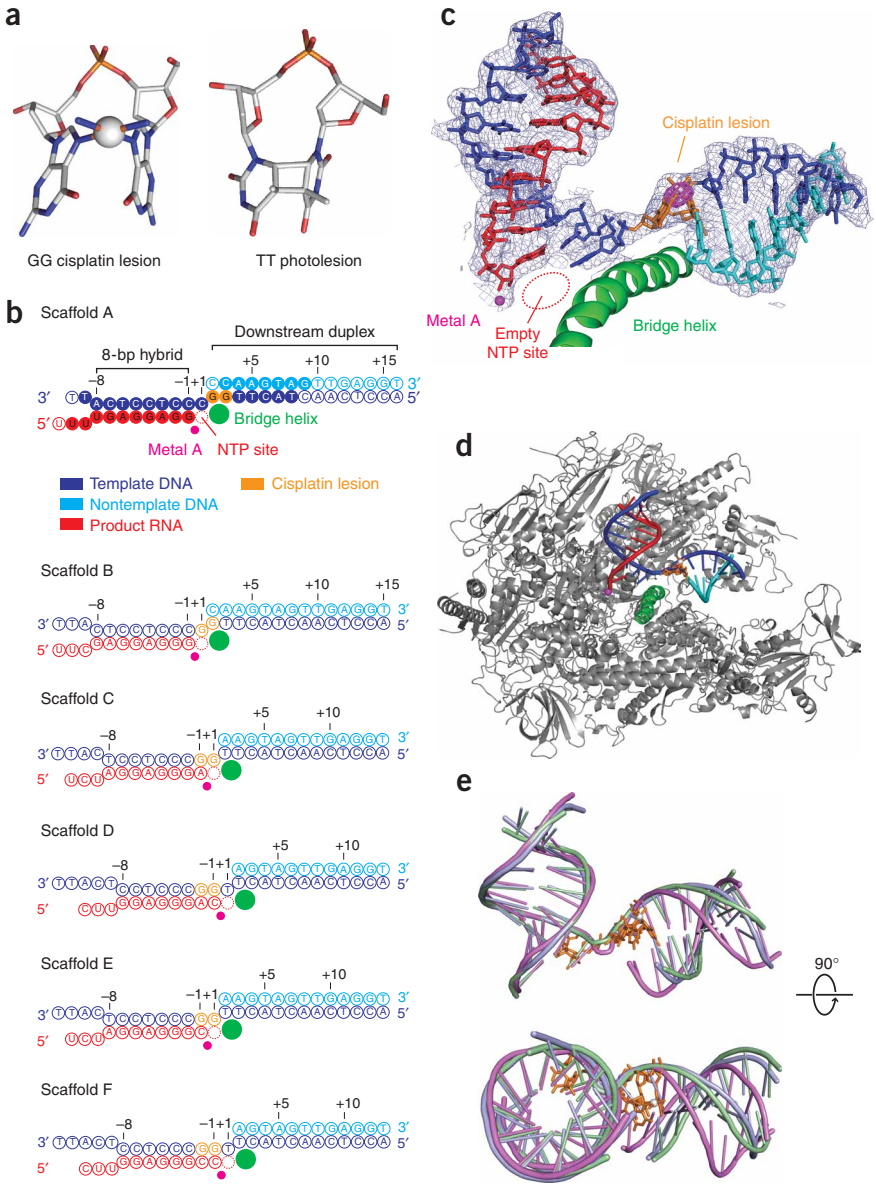

Figure 1 Structure of a cisplatin-damaged Pol II elongation complex. (**a**) The 1,2-d(GpG) intrastrand platinum cross-link (cisplatin lesion) and the TT CPD photolesion. Figures were prepared with PyMOL (http://pymol.sourceforge.net). (**b**) Nucleic acid scaffolds. Filled circles denote nucleotides with interpretable electron density that were included in the structure in **c**; open circles denote nucleotides with uninterpretable or absent electron density. (**c**) Structure of nucleic acids in Pol II elongation complex A. Final $2F_o - F_c$ electron density map for the nucleic acids is shown (blue, contoured at 1.0σ). Anomalous difference Fourier map reveals the location of the platinum atom (magenta, contoured at 15σ). (**d**) Overview of the cisplatin-damaged Pol II elongation complex. Pol II is shown as a silver ribbon, with the bridge helix highlighted in green. The nucleic acids are in color, and the cisplatin lesion is shown as a stick model in orange. A large portion of Pol II was omitted for clarity. (**e**) Cisplatin-induced changes in the downstream DNA. Comparison of the course of nucleic acids in complex A (pale green) with that in the structures of the CPD-containing complexes B and C[8] (violet and light blue, respectively). The proteins were superimposed on the basis of the active site region and then omitted. Nucleic acids are depicted as ribbons, lesions as orange sticks.

the RNA-extension products were separated on polyacrylamide gels and visualized with a fluorimager (**Fig. 2**). After incubation with a physiological concentration of 1 mM NTPs for 20 min, most of the RNA was extended by two nucleotides (**Fig. 2a**). Thus, the complex apparently stalled after nucleotide incorporation opposite the first guanosine (the 3′-guanosine) of the cisplatin lesion. Incubation of complex A with subsets of NTPs suggested that the terminal incorporation is a specific misincorporation of AMP (**Fig. 2a**). To further investigate this, we prepared a scaffold that resulted in an elongation complex that was advanced by one position (scaffold B, **Fig. 1b**). As expected, the results of incubation of complex B with individual NTPs again revealed AMP misincorporation (**Fig. 2a**).

A time course of RNA extension with complex A showed that the first incorporation event was fast, whereas the second incorporation—that is, the apparent misincorporation—was much slower and incomplete (**Fig. 2b**, upper). Apparently, the initial incorporation is fast because GMP is correctly incorporated opposite a template cytidine and because the substrate site is free in complex A (**Fig. 1c**), and translocation of the polymerase is not required. The slow rate of the second incorporation event was confirmed in a time course of RNA extension with complex B (**Fig. 2b**, lower). This misincorporation event also required high ATP concentrations and was not observed in the presence of only 10 μM ATP (**Fig. 2b**).

Possible mechanisms for misincorporation

As the template strand in our scaffold contained a thymidine immediately downstream of the cisplatin lesion, AMP misincorporation may have arisen from template misalignment, a recently characterized mechanism for misincorporation of nucleotides[12]. During misalignment, the cisplatin lesion would transiently adopt a flipped-out, extrahelical conformation, and the thymidine flanking the lesion on the 5′ side would transiently occupy the position of the template base, at register +1 in the active site, to direct AMP incorporation. To test whether this was the case, we prepared a scaffold that was identical to scaffold A except that the flanking thymidine was replaced by cytidine (scaffold $A^{T\rightarrow C}$, **Supplementary Fig. 1** online). This altered scaffold gave rise to the same RNA-extension products (**Fig. 2d**), however, showing that template misalignment did not occur. We confirmed this by altering scaffold B and repeating the RNA-extension assay (**Fig. 2d**).

Another possible explanation for AMP misincorporation is that the 3′-guanosine of the lesion could act as a templating base by adopting a position that allows it to form two hydrogen bonds with the Watson-Crick positions of an incoming ATP substrate (**Fig. 2c**). To test whether the third Watson-Crick position of the 3′-guanosine in the lesion, the extracyclic 2-amino group, is involved in templating AMP misincorporation, we replaced the 3′-guanosine in the lesion with

inosine (I; see Methods), which lacks the 2-amino group (**Fig. 2c** and Methods). RNA-extension analysis showed that AMP was still specifically misincorporated when scaffolds A and B were modified by replacement of the GG cisplatin lesion with an IG cisplatin lesion (**Fig. 2e**). Thus, AMP misincorporation does not involve the 2-amino group. These results were consistent with lesion-templated misincorporation involving a G·A base pair (**Fig. 2c**), but we could not test this directly.

Impaired entry of lesions into the active site

If the AMP misincorporation is templated by the lesion, the lesion must adopt a position in the active site, at least transiently. However,

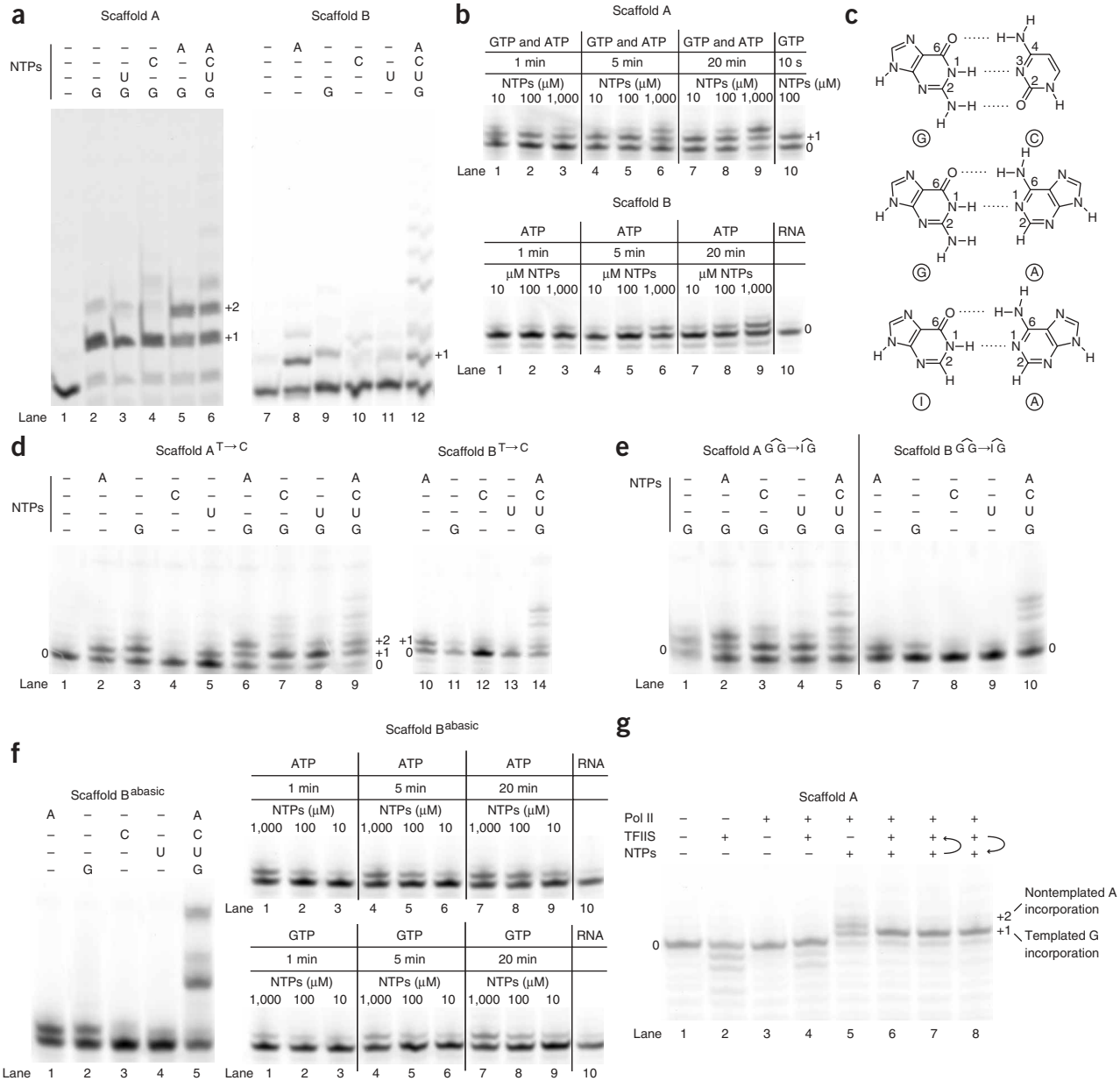

Figure 2 Pol II stalling and misincorporation. (**a**) RNA extension with scaffolds A and B. Lanes 1 and 7 show the fluorescently labeled reactant RNA. In the other lanes, the scaffolds were incubated with Pol II and indicated NTPs (1 mM) for 20 min (see Methods). (**b**) Time courses of the RNA-extension reactions shown in **a** and dependence on NTP concentration. (**c**) Possible base pair formation. Hydrogen bonds are indicated with dashed lines. (**d**) Adenosine misincorporation does not result from template misalignment. Altered scaffolds were used in which the thymidine at the 5′ flanking position of the lesion was replaced by cytidine (compare **Supplementary Fig. 1**). The misincorporation seen in lane 2 is also observed with an undamaged scaffold (**Supplementary Fig. 4** online) and therefore is not due to the lesion. (**e**) The 2-amino group at the 3′ position of the lesion is not involved in directing misincorporation. Altered scaffolds were used in RNA-extension assays in which the guanosine at the 3′ position of the lesion was replaced by inosine. (**f**) Nontemplated purine incorporation at an abasic site. The scaffold used corresponds to scaffold B but contains an abasic site at the templating position +1 and no cisplatin lesion (**Supplementary Fig. 1**). (**g**) Effect of RNA cleavage factor TFIIS on RNA elongation with scaffold A. NTPs and TFIIS were added either simultaneously (lane 6) or sequentially as indicated by arrows, with individual incubation times of 20 min (lanes 7 and 8).

structural considerations suggest that lesion entry into the active site would be impaired, because translocation of the cisplatin dinucleotide lesion from positions +2/+3 to positions +1/+2 is expected to be disfavored, as is the case for a dinucleotide photolesion[8]. Template bases in positions +1/+2 are twisted against each other by about 90° in structures of the undamaged elongation complex[9,13], but such twisting is impossible for nucleotides that are covalently linked in dinucleotide lesions, giving rise to a translocation barrier[8]. To determine whether translocation of the cisplatin lesion is indeed impaired, we crystallized complex B, which was designed to contain the dimer at positions +1/+2 (scaffold B, **Fig. 1b**). The anomalous difference Fourier map revealed a platinum peak at the same location where one was seen in complex A, indicating that the polymerase had apparently stepped backward by one position, so that the cisplatin lesion again occupied positions +2/+3 (**Fig. 3a**). A lower height of the platinum peak (**Supplementary Table 1** online) indicated partial occupancy of the nucleic acids. Indeed, the electron density for the nucleic acids was weak and fragmented, and did not allow for model-building. Thus, the cisplatin lesion was not stably accommodated at positions +1/+2, and translocation from positions +2/+3 to positions +1/+2 was apparently disfavored.

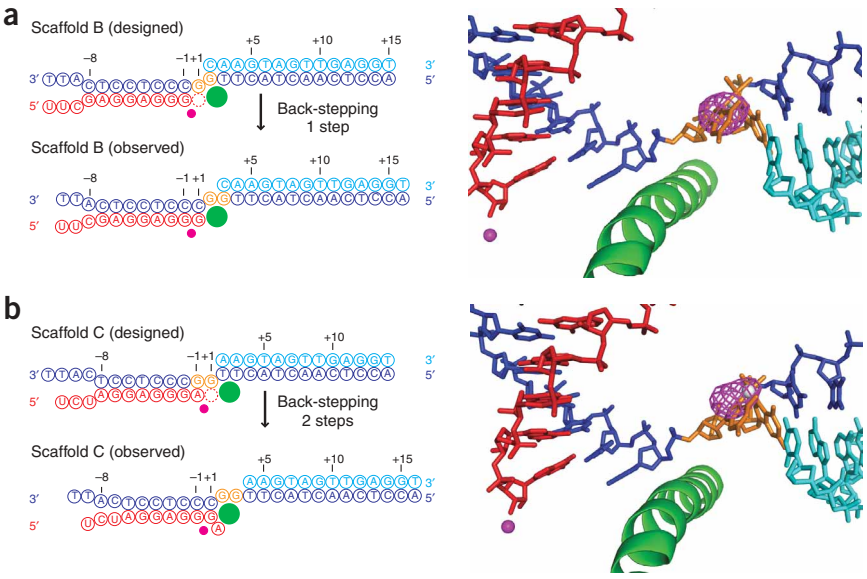

Figure 3 The cisplatin lesion is not stably accommodated in the active site. (**a**,**b**) Anomalous difference Fourier maps of Pol II elongation complexes B (**a**) and C (**b**), contoured at 6σ. Model of complex A is shown, viewed from the side.

These results suggest that the lesion does not stably bind the active site at all. To test this, we prepared a scaffold that contained the lesion at predicted positions –1/+1 in the active site, and a G·A mismatch pair at position –1 (scaffold C, **Fig. 1b**), and crystallized the resulting complex C. The anomalous difference Fourier map revealed a platinum peak at the same location as in complexes A and B, indicating that the polymerase had stepped backward by two positions so that the cisplatin lesion again occupied positions +2/+3 (**Fig. 3b**). The height of the platinum peak was lower than for complexes A and B (**Supplementary Table 1**), and the electron density for the nucleic acids was again fragmented, preventing model-building. We also tried to solve a structure with the lesion placed at positions –2/–1 (scaffold D, **Fig. 1b**). However, crystal structure analysis (**Supplementary Table 1**) revealed no electron density for nucleic acids, consistent with a low affinity of this scaffold for the polymerase. Thus, the cisplatin lesion was not stably accommodated in the active site.

Nontemplated AMP incorporation and an 'A-rule' for Pol II

The crystallographic data strongly suggest impairment of translocation of the lesion to a position where it can direct AMP misincorporation. We therefore asked whether AMP incorporation resulted from nontemplated synthesis. Such preferential, nontemplated AMP incorporation occurs when DNA polymerases encounter a bulky DNA lesion and is known as A-rule[14,15]. We prepared a scaffold identical to scaffold B, but containing an abasic site at the templating position +1 and containing no cisplatin lesion (scaffold B^{abasic}, **Supplementary Fig. 1**). Indeed, AMP, and also to a lesser extent GMP, could be incorporated into RNA opposite the abasic position (**Fig. 2f**), showing that Pol II incorporates purine nucleotides, preferentially AMP, when a templating base is unavailable.

The efficiency of nontemplated AMP incorporation was comparable to that of the terminal AMP misincorporation during stalling at a cisplatin lesion, as judged from the slow rate of the reaction and its dependence on NTP concentration (**Fig. 2b**,**f**). In the presence of the cleavage factor TFIIS, templated GMP incorporation with scaffold A occurred normally, but nontemplated AMP incorporation was suppressed (**Fig. 2g**), consistent with a role of TFIIS in transcriptional proofreading[16,17]. However, TFIIS was unable to promote passage over the translocation barrier.

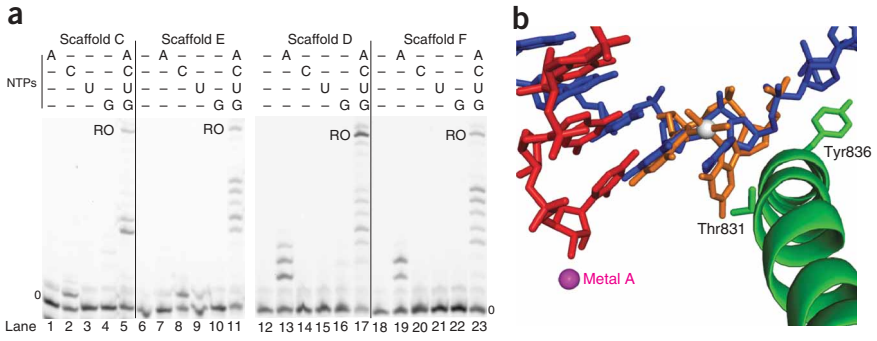

Figure 4 Lesion bypass. (**a**) RNA extension with scaffolds C, D, E and F. Lanes 6, 12 and 18 show the fluorescently labeled reactant RNA. In the other lanes, the scaffolds were incubated with Pol II and indicated NTPs (1 mM) for 20 min (see Methods). Run-off products are indicated (RO). Additional RNA-extension assays confirmed these results (**Supplementary Fig. 5** online). (**b**) Modeling of the cisplatin lesion at positions +1/–1. A cisplatin lesion was manually placed such that it superimposes with template nucleotides at the active center positions +1 and –1 of complex A. Owing to some close contacts, in particular with Thr831 in the bridge helix, slight conformational changes are required to accommodate the lesion.

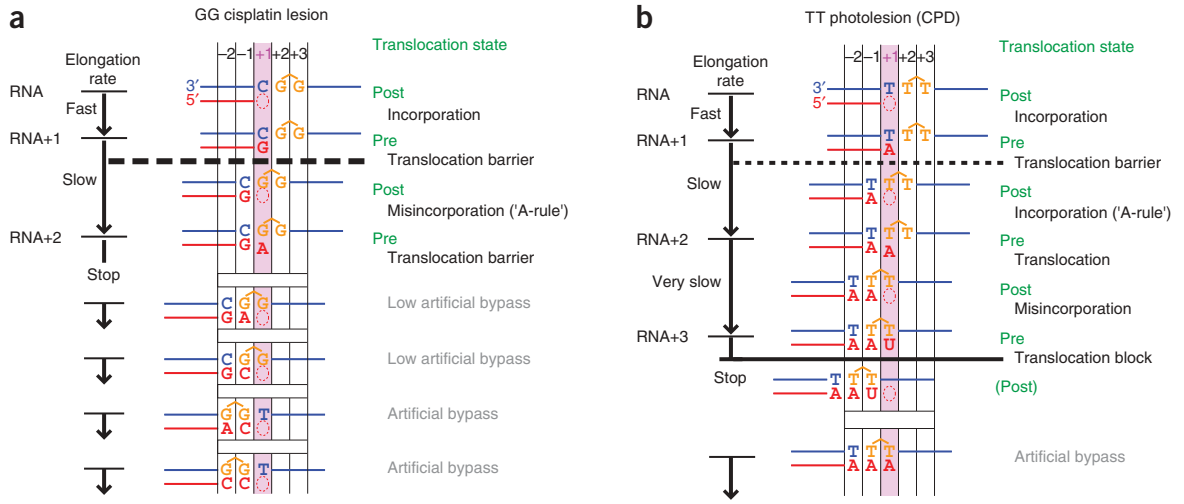

Figure 5 Different mechanisms of Pol II stalling at dinucleotide lesions. (**a**) Pol II stalling at the cisplatin lesion (this study), shown as a schematic representation of RNA extension in complex A. The initial RNA (top) corresponds to the unextended RNA of scaffold A. Dashed line represents translocation barrier. The artificial conditions leading to lesion bypass are depicted at the bottom. (**b**) Pol II stalling at a CPD lesion. Schematic is adapted from reference 8.

Together, these observations suggest that Pol II obeys an 'A-rule' for nontemplated nucleotide addition, which could explain the terminal AMP incorporation when the bulky cisplatin lesion is encountered. This mechanism is consistent with the model in which the cisplatin lesion does not enter the active site during elongation, not even transiently to direct terminal AMP incorporation.

Artificial bypass of a cisplatin lesion

The above data suggest that impaired translocation and delivery of the lesion to the active site causes polymerase stalling, but do not exclude the possibility that stalling is due to the terminal AMP misincorporation and impaired elongation of the resulting G•A mismatch. To test whether polymerase stalling depends on the misincorporation event, we carried out RNA-extension studies with scaffold C, which contained the misincorporated adenosine opposite the 3′-guanosine of the cisplatin lesion, and with a scaffold that contained the cognate cytidine at this position (scaffold E, **Fig. 1b**). Incubation of complexes C and E with individual NTPs showed that CMP was correctly incorporated opposite the 5′-guanosine of the lesion, although AMP misincorporation also occurred, albeit less efficiently (**Fig. 4a**). The majority of elongation complexes C and E did not allow for RNA extension past the lesion (**Fig. 4a**), indicating that they are stably stalled and that stalling is independent of the G•A mismatch. Thus, misincorporation is not required for stalling.

Prolonged incubation of scaffolds C and E with Pol II and NTPs, however, led to a small but reproducible amount of run-off products (**Fig. 4a**). These products may be a result of lesion bypass. Alternatively, they may arise from deplatination of the DNA, maybe by transfer of the platinum to an amino acid side chain of Pol II. To investigate this, we analyzed the nucleic acid products resulting from prolonged incubation of complex A with Pol II and NTPs by MALDI mass spectrometry. Only intact, fully platinated template strand was observed (**Supplementary Fig. 2** online), and this represents strong evidence against deplatination. Thus, the cisplatin lesion apparently can occupy the active site transiently if a nucleotide is present in the RNA opposite the 3′-guanosine of the lesion, enabling RNA extension past the lesion for a fraction of complexes. Modeling showed that entry of the bulky cisplatin lesion into the active site would require conformational changes but that the lesion, once entered, could be accommodated in the active site with only slight structural changes (**Fig. 4b**).

To provide further support for possible lesion bypass, we used scaffolds in which the RNA contained nucleotides opposite both guanosines of the cisplatin lesion (scaffolds D and F, **Fig. 1b**). Incubation of the resulting elongation complexes with NTPs gave rise to efficient lesion bypass (**Fig. 4a**). Notably, bypass was possible not only with a G-C match at the 3′ position of the lesion, but also with a G•A mismatch at this position (**Fig. 4a**). These data show that lesion bypass is facilitated by RNA nucleotides that are already present in the scaffold opposite the lesion, most probably because this facilitates binding of the lesion beyond the translocation barrier, at positions –2/–1, just upstream of the active site. Because Pol II can pass the lesion and a mismatch, stalling is not due to impaired extension of a lesion-containing hybrid or a mismatch. This supports the model in which stalling results from impaired translocation and entry of the lesion into the active site.

DISCUSSION

In the structural and functional studies described here, we used cisplatin lesion–containing Pol II elongation complexes to investigate the detailed mechanism of transcriptional stalling at the most frequent cisplatin-induced DNA adduct. We show that Pol II stalls in front of a cisplatin lesion because it does not pass a translocation barrier that impairs delivery of the bulky lesion into the active site. When elongation complexes are prepared in which the lesion is positioned beyond the translocation barrier, bypass of the lesion is possible.

To our surprise, stalled Pol II was able to incorporate AMP in an apparently nontemplated manner according to an A-rule that has been described previously for DNA polymerases[14,15]. The A-rule may explain inefficient AMP incorporation not only at the cisplatin lesion, but also at the same position during transcription of another dinucleotide lesion, the TT CPD photolesion[8]. This model supersedes the non-intuitive assumption that when CPD enters the active site, its 3′-thymidine acts as a template to direct AMP incorporation. AMP incorporation according to an A-rule enables formation of a matched

T-A base pair at the 3′ position of the CPD, and this may stabilize the lesion in the active site[8]. In contrast, at the 3′ position of the cisplatin lesion, A-rule incorporation would result in a G•A mismatch if the lesion were able to cross the translocation barrier. Pol II bypassed the cisplatin lesion and the mismatch when they were artificially placed beyond the translocation barrier, showing that the barrier prevents efficient transcriptional mutagenesis and synthesis of substantial amounts of erroneous RNAs.

Comparison of the results with the previously established mechanism of Pol II stalling at a CPD[8] reveals that Pol II stalls at the two dinucleotide lesions for different reasons (**Fig. 5**). First, the cisplatin lesion cannot overcome the translocation barrier, but the CPD can, and the CPD binds in the active site. Second, inefficient AMP incorporation occurs at both lesions, but it enables lesion binding at the active site positions –1/+1 only for the CPD, probably because a stabilizing T-A base pair is formed at position –1, in contrast to a G•A mismatch that would be formed at the cisplatin lesion. Third, UMP misincorporation occurs opposite the 5′ nucleotide of the CPD, whereas correct incorporation occurs opposite the 5′ nucleotide of the cisplatin lesion, but only if the lesion is artificially placed beyond the translocation barrier. Fourth, AMP misincorporation at the cisplatin lesion is not required for stalling, but CPD-directed UMP misincorporation is required for stalling. Finally, the misincorporated nucleotide opposite the cisplatin lesion can be bypassed, whereas the misincorporated nucleotide opposite the CPD cannot.

Thus, the detailed mechanisms of transcriptional stalling at two different dinucleotide lesions differ in many respects. As a consequence, it is impossible to predict the mechanisms of transcriptional stalling or mutagenesis at other types of lesions. Instead, the detailed stalling mechanisms remain to be investigated for other lesions, including the less frequent 1,3-d(GpNpG) intrastrand platinum cross-link[6,7,18,19]. Nevertheless, this study and our previous study of CPD-induced transcriptional stalling[8] suggest general aspects of the recognition of bulky dinucleotide lesions by Pol II, including a translocation barrier between positions +2/+3 and +1/+2, an A-rule for nontemplated nucleotide incorporation, and the possibility of lesion bypass under conditions that circumvent the natural stalling mechanism.

METHODS

Sample preparation. Endogenous ten-subunit *S. cerevisiae* Pol II core enzyme was purified as described[20] except that the anion-exchange step was omitted. Recombinant TFIIS was prepared as described[9], and synthetic oligonucleotides were annealed for scaffold assembly as described[8]. We assembled Pol II–nucleic acid scaffold complexes by incubating pure core Pol II with two molar equivalents of nucleic acid scaffold in transcription buffer (20 mM HEPES (pH 7.6), 60 mM $(NH_4)_2SO_4$, 8 mM $MgSO_4$, 10 μM $ZnCl_2$, 10% (v/v) glycerol, 10 mM DTT) at 20 °C for 30 min as described[8]. DNA strands containing the 1,2-d(GpG) and 1,2-(IpG) cisplatin intrastrand cross-links were synthesized as described[11].

RNA extension and cleavage assays. Pol II–nucleic acid scaffold complex (5 pmol) was incubated at 28 °C for 20 min with 1 mM NTPs in transcription buffer for RNA extension, or with 10 pmol TFIIS for RNA cleavage, unless mentioned otherwise. For gel electrophoresis, reactions were stopped by addition of an equal volume of 2× urea loading buffer (8 M urea, 2× Tris-Borate-EDTA buffer) and incubation for 5 min at 95 °C. For electrophoresis, the denatured reaction mixture corresponding to 0.5 pmol Pol II was loaded and 6-carboxyfluoresceine (FAM) 5′ end–labeled RNA products were visualized with a Typhoon 9400 scanner (GE Healthcare). For MALDI-TOF analysis, reactions were incubated overnight with 1 mM NTPs, stopped and analyzed as described[8].

Table 1 Crystallographic data and refinement statistics

	Pol II elongation complex with cisplatin lesion
Data collection	
Space group	$C222_1$
Cell dimensions	
a, *b*, *c* (Å)	222.1, 393.1, 283.7
Resolution (Å)	50.0–3.80 (4.02–3.80)
R_{sym}	8.8 (36.2)
$I / \sigma I$	11.2 (3.4)
Completeness (%)	99.1 (97.0)
Redundancy	3.4 (3.2)
Refinement	
Resolution (Å)	50.0–3.80
No. reflections	235,052
R_{work} / R_{free}[a]	21.5 / 24.0
No. atoms	
Protein	31,102
Nucleic acids	698
B-factors	
Protein	115.5
Nucleic acids	144.0
R.m.s. deviations	
Bond lengths (Å)	0.008
Bond angles (°)	1.5
Platinum peak in anomalous difference Fourier (σ)	23.5

Structure was determined for elongation complex A (scaffold A with cisplatin lesion at positions +2/+3). Diffraction data were collected from a single crystal. Values in parentheses are for the highest-resolution shell.
[a]For free R-factor calculation, we excluded from refinement the same set of reflections that had been excluded from previous Pol II structure determinations[8,9,24].

Crystal structure analysis. The cisplatin lesion–containing scaffolds were cocrystallized and the structures were determined essentially as described[8,9], with minor changes. Stoichiometric Pol II–scaffold complexes were assembled by incubating core Pol II for 10 min with two molar equivalents of nucleic acid scaffold, then incubating this mixture for 20 min with five molar equivalents of recombinant Rpb4-Rpb7 in Pol II buffer (5 mM HEPES (pH 7.25), 40 mM $(NH_4)_2SO_4$, 10 μM $ZnCl_2$, 10 mM DTT) at 20 °C. The complexes were purified by size-exclusion chromatography (Superose 6 10/300 GL) in Pol II buffer. We grew crystals at 22 °C with the hanging drop vapor diffusion method, by mixing 2 μl of sample solution with 1 μl of reservoir solution (200 mM ammonium acetate, 150 mM magnesium acetate, 50 mM HEPES (pH 7.0), 5% (w/v) PEG 6,000, 5 mM Tris(2-carboxyethyl) phosphine (TCEP)). Diffraction data were collected at a wavelength of 1.0716 Å at the protein crystallography beamline X06SA of the Swiss Light Source (**Table 1** and **Supplementary Table 1**). Raw data were processed with XDS[21] or DENZO[22] (complex B). Structures were solved by molecular replacement with the program Phaser[23], using the structure of the complete 12-subunit Pol II[24]. The molecular-replacement solution was subjected to rigid-body refinement with CNS[25]. Model-building was done with O[26] and Coot[27]. The nucleic acids were built stepwise into unbiased $F_o - F_c$ electron density maps (**Supplementary Fig. 3** online). CNS topologies for the cisplatin lesion were obtained with XPLO2D (http://xray.bmc.uu.se/usf/xplo2d_man.html). Refinement was monitored with the free *R*-factor, calculated from the same set of excluded reflections as in the refinement of the complete Pol II complex[24] and the complete Pol II elongation complex[8,9].

Accession codes. Protein Data Bank: Coordinates and structure factors have been deposited with accession code 2R7Z.

Note: Supplementary information is available on the Nature Structural & Molecular Biology website.

ACKNOWLEDGMENTS

We thank members of the Cramer laboratory for help. P.C. and T.C. were supported by the Deutsche Forschungsgemeinschaft, the Sonderforschungsbereich SFB646 and the Fonds der chemischen Industrie. P.C. was supported by the EU grant 3D repertoire, contract no. LSHG-CT-2005-512028. G.E.D. and F.B. were supported by the Elite Netzwerk Bayern. A.A. was supported by the Marie Curie training and mobility network CLUSTOX DNA.

AUTHOR CONTRIBUTIONS

G.E.D. performed and analyzed biochemical and crystallographic experiments. A.A. synthesized cisplatin-containing DNA strands and performed MALDI experiments. F.B. assisted with experiments and crystallography. T.C. supervised the project. P.C. supervised the project and wrote the manuscript.

Published online at http://www.nature.com/nsmb/
Reprints and permissions information is available online at http://npg.nature.com/reprintsandpermissions

1. Wang, D. & Lippard, S.J. Cellular processing of platinum anticancer drugs. *Nat. Rev. Drug Discov.* **4**, 307–320 (2005).
2. Kartalou, M. & Essigmann, J.M. Recognition of cisplatin adducts by cellular proteins. *Mutat. Res.* **478**, 1–21 (2001).
3. Jung, Y. & Lippard, S.J. Multiple states of stalled T7 RNA polymerase at DNA lesions generated by platinum anticancer agents. *J. Biol. Chem.* **278**, 52084–52092 (2003).
4. Corda, Y., Job, C., Anin, M.F., Leng, M. & Job, D. Transcription by eucaryotic and procaryotic RNA polymerases of DNA modified at a d(GG) or a d(AG) site by the antitumor drug cis-diamminedichloroplatinum(II). *Biochemistry* **30**, 222–230 (1991).
5. Corda, Y., Job, C., Anin, M.F., Leng, M. & Job, D. Spectrum of DNA-platinum adduct recognition by prokaryotic and eukaryotic DNA-dependent RNA polymerases. *Biochemistry* **32**, 8582–8588 (1993).
6. Tornaletti, S., Patrick, S.M., Turchi, J.J. & Hanawalt, P.C. Behavior of T7 RNA polymerase and mammalian RNA polymerase II at site-specific cisplatin adducts in the template DNA. *J. Biol. Chem.* **278**, 35791–35797 (2003).
7. Jung, Y. & Lippard, S.J. RNA polymerase II blockage by cisplatin-damaged DNA. Stability and polyubiquitylation of stalled polymerase. *J. Biol. Chem.* **281**, 1361–1370 (2006).
8. Brueckner, F., Hennecke, U., Carell, T. & Cramer, P. CPD damage recognition by transcribing RNA polymerase II. *Science* **315**, 859–862 (2007).
9. Kettenberger, H., Armache, K.-J. & Cramer, P. Complete RNA polymerase II elongation complex structure and its interactions with NTP and TFIIS. *Mol. Cell* **16**, 955–965 (2004).
10. Gelasco, A. & Lippard, S.J. NMR solution structure of a DNA dodecamer duplex containing a cis-diammineplatinum(II) d(GpG) intrastrand cross-link, the major adduct of the anticancer drug cisplatin. *Biochemistry* **37**, 9230–9239 (1998).
11. Takahara, P.M., Rosenzweig, A.C., Frederick, C.A. & Lippard, S.J. Crystal structure of double-stranded DNA containing the major adduct of the anticancer drug cisplatin. *Nature* **377**, 649–652 (1995).
12. Kashkina, E. *et al.* Template misalignment in multisubunit RNA polymerases and transcription fidelity. *Mol. Cell* **24**, 257–266 (2006).
13. Gnatt, A.L., Cramer, P., Fu, J., Bushnell, D.A. & Kornberg, R.D. Structural basis of transcription: an RNA polymerase II elongation complex at 3.3 Å resolution. *Science* **292**, 1876–1882 (2001).
14. Strauss, B.S. The 'A rule' of mutagen specificity: a consequence of DNA polymerase bypass of non-instructional lesions? *Bioessays* **13**, 79–84 (1991).
15. Taylor, J.S. New structural and mechanistic insight into the A-rule and the instructional and non-instructional behavior of DNA photoproducts and other lesions. *Mutat. Res.* **510**, 55–70 (2002).
16. Wind, M. & Reines, D. Transcription elongation factor SII. *Bioessays* **22**, 327–336 (2000).
17. Thomas, M.J., Platas, A.A. & Hawley, D.K. Transcriptional fidelity and proofreading by RNA polymerase II. *Cell* **93**, 627–637 (1998).
18. Tremeau-Bravard, A., Riedl, T., Egly, J.M. & Dahmus, M.E. Fate of RNA polymerase II stalled at a cisplatin lesion. *J. Biol. Chem.* **279**, 7751–7759 (2004).
19. Laine, J.P. & Egly, J.M. Initiation of DNA repair mediated by a stalled RNA polymerase IIO. *EMBO J.* **25**, 387–397 (2006).
20. Armache, K.-J., Kettenberger, H. & Cramer, P. Architecture of the initiation-competent 12-subunit RNA polymerase II. *Proc. Natl. Acad. Sci. USA* **100**, 6964–6968 (2003).
21. Kabsch, W. Automatic processing of rotation diffraction data from crystals of initially unknown symmetry and cell constants. *J. Appl. Cryst.* **26**, 795–800 (1993).
22. Otwinowski, Z. & Minor, W. Processing of X-ray diffraction data collected in oscillation mode. *Methods Enzymol.* **276**, 307–326 (1996).
23. McCoy, A.J., Grosse-Kunstleve, R.W., Storoni, L.C. & Read, R.J. Likelihood-enhanced fast translation functions. *Acta Crystallogr. D Biol. Crystallogr.* **61**, 458–464 (2005).
24. Armache, K.-J., Mitterweger, S., Meinhart, A. & Cramer, P. Structures of complete RNA polymerase II and its subcomplex Rpb4/7. *J. Biol. Chem.* **280**, 7131–7134 (2005).
25. Brunger, A.T. *et al.* Crystallography & NMR system: a new software suite for macromolecular structure determination. *Acta Crystallogr. D Biol. Crystallogr.* **54**, 905–921 (1998).
26. Jones, T.A., Zou, J.Y., Cowan, S.W. & Kjeldgaard, M. Improved methods for building protein models in electron density maps and the location of errors in these models. *Acta Crystallogr. A* **47**, 110–119 (1991).
27. Emsley, P. & Cowtan, K. Coot: model-building tools for molecular graphics. *Acta Crystallogr. D Biol. Crystallogr.* **60**, 2126–2132 (2004).